Energy-Efficient Wi-Fi Sensing Policy Under Generalized Mobility Patterns With Aging

Jaeseong Jeong, Yung Yi, Jeong-Woo Cho, Do Young Eun, *Senior Member, IEEE*, and Song Chong, *Member, IEEE*

***Abstract*—An essential condition precedent to the success of mobile applications based on Wi-Fi (e.g., iCloud) is an energy-efficient Wi-Fi sensing. Clearly, a good Wi-Fi sensing policy should factor in both inter-access point (AP) arrival time (IAT) and contact duration time (CDT) distributions of each individual. However, prior work focuses on limited cases of those two distributions (e.g., exponential) or proposes heuristic approaches such as Additive Increase (AI). In this paper, we first formulate a generalized functional optimization problem on Wi-Fi sensing under general inter-AP and contact duration distributions and investigate how each individual should sense Wi-Fi APs to strike a good balance between energy efficiency and performance, which is in turn intricately linked with users mobility patterns. We then derive a generic optimal condition that sheds insights into the aging property, underpinning energy-aware Wi-Fi sensing polices. In harnessing our analytical findings and the implications thereof, we develop a new sensing algorithm, called Wi-Fi Sensing with AGing (WiSAG), and demonstrate that WiSAG outperforms the existing sensing algorithms up to 37% through extensive trace-driven simulations for which real mobility traces gathered from hundreds of smartphones is used.**

***Index Terms*—Aging, energy efficiency, functional optimization, Wi-Fi sensing.**

I. Introduction

A. Motivation

THE NUMBER of mobile users with smartphones/pads is rapidly increasing. Cisco reported that mobile data traffic grew 2.6-fold in 2010, and forecasts that it will increase 26-fold between 2010 and 2015 [1]. Smarter applications generating heavier traffic are expediting the scarcity of 3G capacity. 4G, which has started to be deployed, seems to be only a temporary solution due to huge difference between traffic demands and available physical resources in the cellular system.

Leveraging Wi-Fi is an intriguing solution that has high potential in alleviating mobile data explosion. The very feature of shorter-range communication of Wi-Fi than that of 3G or 4G on the unlicensed bands brings considerable efficiency in spatial frequency reuse. Wi-Fi access points (APs)[1] also cost much less than cellular base stations [2], so that they can be deployed quickly as well as without heavy financial burden to operators and even users. In fact, Wi-Fi APs have already been installed around hotspots in many countries now. Very lately, researchers have started to examine the effect of Wi-Fi offloading from the theoretical and experimental perspectives [2]–[4]. For example, Lee *et al.* [2] showed that about 70% cellular data can be offloaded to Wi-Fi if users would tolerate 2-h delayed data delivery. Wi-Fi is particularly useful for applications that periodically exploit the network, e.g., iCloud [5] and Microsoft Pocket Outlook [6]. Urban Tomography System [7] allows users to capture video clips, and then automatically uploads them to a server via Wi-Fi. Wi-Fi connectivity can also provide the location information, whose economic value is huge [8].

Yet, not every user seems to welcome Wi-Fi. The survey by Devicescape [9] tells us that 64% of US consumers hit hotspots at least once a day, but some of them sometimes spend a day without Wi-Fi connections. From mobile users' perspective, one of the biggest concerns lies in quick battery discharge by Wi-Fi sensing [10]–[16]. It is reported [17] that 41% of iPhone 3G users and 15% of iPhone 4 users mention such a battery concern. Also, Wi-Fi-equipped wearable devices and sensors for Internet of Things (IoT) whose markets are rapidly growing severely suffer from the lack of battery capacity due to their size limitation. Therefore, in order to maximally exploit Wi-Fi's benefits, it is essential to relax users' attention to battery drainage by developing energy-efficient sensing schemes that sense scattered APs while sparingly using mobiles' batteries.

B. Summary and Main Contributions

In order to design the "best" Wi-Fi sensing scheme, we can gather that there exists a fundamental tradeoff between energy efficiency and performance: Sensing with less frequency results in bigger energy saving, but entails lower chances of data transmission through Wi-Fi. To strike a good balance, two key factors from a user's mobility pattern need to be carefully addressed: 1) how often users meet APs [referred to as *inter-AP arrival*

Manuscript received May 11, 2014; revised December 01, 2014 and July 12, 2015; accepted July 13, 2015; approved by IEEE/ACM TRANSACTIONS ON NETWORKING Editor S. Puthenpura. This work was supported in part by the Institute for Information & communications Technology Promotion (IITP) Grant funded by the Korea Government (MSIP) (B0126-15-1078), the ICT R&D program of MSIP/IITP (14-000-04-001), the International Research & Development Program of the National Research Foundation of Korea (NRF) funded by MSIP (K2013078191), the Seventh Framework Programme (FP7) funded by the European Commission (611165), and the National Science Foundation under Grants CNS-1217341 and CNS-1423151. The work of J. Jeong was supported by ERC and VR grants.

J. Jeong is with the Automatic Control Department, KTH Royal Institute of Technology, 10044 Stockholm, Sweden (e-mail: jaeseong@kth.se).

Y. Yi and S. Chong are with the Department of Electrical Engineering, Korea Advanced Institute of Science and Technology (KAIST), Daejeon 305-701, Korea (e-mail: yiyung@kaist.edu, songchong@kaist.edu).

J.-W. Cho is with the School of Information and Communication Technology, KTH Royal Institute of Technology, 16440 Kista, Sweden (e-mail: jwcho@kth.se).

D. Y. Eun is with the Department of Electrical and Computer Engineering, North Carolina State University, Raleigh, NC 27695 USA (e-mail: dyeun@ncsu.edu).

Color versions of one or more of the figures in this paper are available online at http://ieeexplore.ieee.org.

Digital Object Identifier 10.1109/TNET.2015.2468590

[1]We simply use "AP" throughout this paper.

time (IAT)], and 2) how long a user is in contact with an AP (called *AP contact duration time*).

Prior work [18], [13] studied optimal sensing intervals for only limited cases, e.g., exponential inter-AP arrivals and contact durations, in which periodic sensing interval is optimal. They also introduced heuristic algorithms such as Additive Increase (AI) [18] and WiFisense [13], both of which propose to increase the sensing intervals whenever they fail to detect an AP. However, the following questions still remain: 1) What is an optimal sensing policy for the users who do not have memoryless exponential inter-AP arrivals and contact duration distributions? 2) When do the heuristic algorithms that increase sensing intervals for AP meeting failures work well? These questions are of significant importance because, as discussed in Section VI, users have diverse mobility patterns, thus diverse distributions on inter-AP arrival and contact duration times.

To answer the questions above, we take a *holistic* approach by formulating a mathematical problem that captures a user's mobility pattern under general distributions of inter-AP arrival and contact duration time, and the tradeoff between energy consumption and contact loss. More formally, we adopt a functional optimization approach, where our objective is to minimize a linear scalarization[2] of energy consumption and contact loss, both of which are functions of sensing process over time. By computing a necessary condition for optimality, which is also sufficient under mild cases, we first find that the key factor to how we should sense APs optimally is simply the *aging property* of an inter-AP arrival time, for a given AP contact duration distribution. The notion of aging property is from reliability theory [20], intuitively explained as follows: Consider an event that a mobile node has not been in contact with an AP until time x. We say that aging of the inter-AP arrival time is positive (resp. negative) if when x increases, the remaining time to meet an AP from x, stochastically decreases (resp. increases). Analysis through the aging concept extremely simplifies the understanding of the "best" sensing process, providing diverse practical implications. Our theoretical study reveals how sensing intervals should be chosen depending on a user's *diverse* mobility patterns measured by inter-AP arrival and contact duration distributions, as summarized in Table I. Also, we compute the optimality condition under another type of objective that minimizes a linear-fractional scalarization[3] of energy consumption and contact loss, and show that the dependency structure between the optimal sensing process and mobility patterns in Table I also holds. From the theory-driven implications, we develop a new sensing algorithm, called Wi-fi Sensing with AGing (WiSAG), which adaptively varies sensing intervals depending on the features of inter-AP arrival and contact duration times.

In order to study the distributions of inter-AP arrivals and contact durations of real users and evaluate the performance of WiSAG, we analyze Wi-Fi connectivity logs from the two different traces: 1) 84 3G/3GS iPhone users for 18 days where users are recruited from an iPhone user community in South Korea [2], and 2) 63 students in the Korea Advanced Institute of Science and Technology (KAIST) campus using Android smartphones for 14 days. Both traces reveal that a large fraction of participants have a negative aging property, which claim that their mobiles should sleep longer as the elapsed time from the last AP contact increases. This shows the case when the heuristic algorithms such as AI may work well. However, from our simulations, WiSAG outperforms even AI by up to about 30% on average because better parameter selection, e.g., amount of increasing intervals, can be made in WiSAG than AI. We also observe the relatively regular AP contact patterns from several users who have a positive aging in their distributions. In this case, optimal sensing interval should decrease over time from our theoretical findings. Thus, the existing sensing algorithms [13], [18] that increase sensing intervals fail to achieve high performance, showing about 47% performance gap on average. The key performance improvement over existing algorithms lies in the ability that our theory-inspired algorithm, WiSAG, provides a macroscopic guideline on sensing intervals, i.e., increase or decrease, and further proposes more exact amount of intervals.

TABLE I
KEY FINDINGS FOR SENSING INTERVAL. OUR NEW FINDINGS: **BOLD-FACE**

Contact duration	*Inter-AP arrival (aging)*		
	Negative	Constant	Positive
Weibull Generalized Pareto	***increase***	periodic [18]	***decrease***
Exponential	***increase***	periodic [13], [18]	***decrease***

C. Related Work

There have been many studies on energy-efficient Wi-Fi sensing [13]–[16], [18] based on the Wi-Fi sleep mode. Wi-Fi sensing policies using surrounding information include cellular fingerprint [14], Zigbee [15], accelerometer [13], and Bluetooth logs [16], where the fact that the information is closely correlated to Wi-Fi AP contacts is exploited. However, utilizing that information incurs additional overheads, e.g., battery consumption for collecting the informations [10] and additional resource usage for maintaining and processing the information [14]. Despite the research results that those algorithms are efficient in sensing in several practical scenarios, there may exist some cases where: 1) the available surrounding information is sparsely encountered; 2) the additional overheads become a crucial part; 3) the uncertainty of estimating an AP contact time is still high even with those surrounding information. Thus, considering the randomness of AP contact patterns without explicit support from surrounding information can also be an essential part of WiFi sensing. In fact, most of current smartphones do not use the surrounding informations in AP sensing, but sense only on-demand [13] for saving energy. This paper provides key guidelines to choose sensing intervals and proposes an energy-efficient sensing algorithm under a random AP contact patterns, where such a "blind sensing"[4] is expected to still be important in smartphones.

[2]In multiobjective optimization where both energy consumption and contact loss should be minimized, scalarization is a method to convert a vector of multiple objectives to a scalar value to be optimized [19]. Linear scalarization means a weighted sum of multiple objectives.

[3]Linear-fractional scalarization means a fraction where the numerator and denominator are linear combinations of energy consumption and contact loss, respectively. In this paper, the linear-fractional scalarization of energy consumption and contact loss represents sensing energy per transmission bit.

[4]In this paper, we define "blind sensing" as a sensing scheme which does not use any of surrounding information.

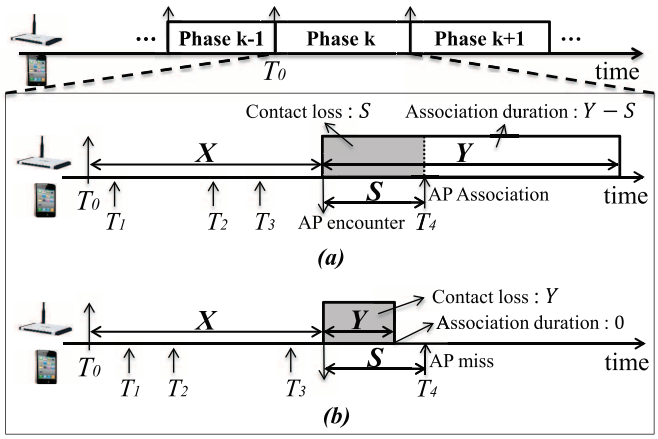

Fig. 1. Illustration of the model. (a) When AP contact duration Y is larger than S, a mobile successfully detects an AP. (b) When AP contact duration Y is smaller than S, a mobile node fails to detect it. Shaded areas denote the contact loss time $l(S)$.

II. Model and Objective

A. System Model

Phases: Mobile nodes (or simply mobiles) move over time and intermittently meet Wi-Fi APs. We divide the entire time into a sequence of *phases*, where a phase corresponds to a time interval ranging from: 1) the instant when a mobile node loses a Wi-Fi contact, and 2) to the end of the next Wi-Fi contact, as depicted in Fig. 1.

Inter-AP Arrival and Contact Duration: Each phase is split into two intervals of when a mobile is not under Wi-Fi coverage, i.e., inter-AP arrival time (IAT), and when a mobile is under Wi-Fi coverage, i.e., AP contact duration time (CDT). We say that a mobile *encounters* an AP when it starts to be under the coverage of an AP. We also say that the mobile *is associated* with an AP when a mobile is aware of being under the AP's coverage, and ready for data transmission at the average rate of r_w. Denote by X and Y the random variables of inter-AP arrival and contact duration times, respectively. Let $F_X(x) = \mathbb{P}[X < x]$ and $F_Y(y) = \mathbb{P}[Y < y]$, and we use $\bar{F}_X(x) = 1 - F_X(x)$ and $\bar{F}_Y(y) = 1 - F_Y(y)$. We assume that phases are independent, i.e., X and Y are i.i.d. across phases, which enables us to focus on a single phase. Due to the recent papers [2], [21], and [22], it has been shown that humans' movement patterns are highly regular. Thus, we assume that each mobile knows its distributions of inter-AP arrival and contact duration times.

Sensing: As depicted in Fig. 1, let T_0 be the starting time of a phase, and a mobile senses APs at times $T_1, T_2, \ldots$. A sequence $(T_k)_{k=1}^{\infty}$ is randomly generated by a sensing process $N(t)$, which is a *nonhomogeneous* Poisson process with rate $n(t)$. Since $n(t)$ may take the form of a pulse train of Dirac delta measures, called *Dirac comb*, $N(t)$ can model deterministic sensing as well as stochastic one. Let c_{s} be the sensing cost, i.e., power consumption per one sensing operation. We assume that mobiles stop sensing after being associated. We also assume that the mobile is able to detect the end of each contact immediately after being outside of Wi-Fi coverage. This assumption is reasonable since the connection loss can be quickly detected if some data transmission is in progress. For the case where a mobile misses a contact due to its large sensing interval, we will it discuss later in Section V.

Loss Time: Note that a mobile can be associated with an AP some time after encountering the AP [time T_4 in Fig. 1(a)]. Let a random variable S be the elapsed time until the next sensing since encountering. We are interested in the *loss time* that quantifies the duration that a mobile node misses the chance to use an AP. In Fig. 1(a), a mobile senses while being in the AP's coverage, where the loss time is S. However, in Fig. 1(b), the mobile moves fast, resulting in missing the AP contact, in which case the loss time is Y. Thus, the average loss time $l(S)$ (with respect to the contact duration Y) is

$$l(S) = \mathbb{E}_Y[\min\{Y, S\}]. \tag{1}$$

B. Problem Formulation

Sensing with less frequency saves larger energy, which in turn increases the chance to miss Wi-Fi contacts, hence lower performance. We set a *functional* optimization problem with a *single* objective that combines energy efficiency with performance in a linear fashion, where one metric is treated as a penalty term. To be more specific, the optimization problem is to minimize the average sensing cost, linearly penalized by missed Wi-Fi contacts, over all feasible sensing policy $N(t)$. By doing so, two conflicting objectives of energy efficiency and performance can be appropriately considered in the formulation.

Minimize sensing cost penalized by lost Wi-Fi contacts

$$\min_{(n(t))_{t=0}^{\infty}} \{c_{\mathrm{s}}\mathbb{E}[N(X)] + \gamma r_w \mathbb{E}[l(S)]\} \tag{OPT}$$

where γ is a penalty weight for the contact loss.

Recall that $\mathbb{E}[N(X)]$ is the average number of sensings before the mobile encounters an AP, and $r_w\mathbb{E}[l(S)]$ corresponds to the average volume of data that cannot be transmitted due to the "lazy" association to the AP. Optimizing a linearly weighted objective function as in (OPT) is a widely adopted approach to encapsulate various tradeoffs of performance metrics in networking community, e.g., in [23] and [24]. γ is a weight of the linear combination representing the amount of average sensing cost to which each unit average contact loss is supposedly translated. In plain words, it can be determined by how *highly* each mobile (or an application within the mobile) attempts to access Wi-Fi *values* contact loss in terms of sensing energy.

Then, our main interest is now centered on minimizing (OPT) by generating the random sequence $(T_k)_{k=0}^{\infty}$ (or choosing $n(t)$ for *every* $t \in (0, \infty)$), and thereby determining the nonhomogeneous Poisson process $N(t)$, where $F_X(\cdot)$ and $F_Y(\cdot)$ are given. We first epitomize the notion of *aging* that will be frequently used in many parts of the discussion throughout this paper.

C. Preliminary: Aging

We define a failure rate [20] that quantifies the probability that a r.v. X (e.g., inter-AP arrival time in our case) is some value, say t, on the condition that $X \geq t$ (e.g., a mobile does not meet an AP until time t).

Definition 1: Consider a r.v. X with the probability density function (PDF) and cumulative distribution function (CDF) of

$f_X(t)$ and $F_X(t)$, respectively. The failure rate $r_X(t)$ of X is: $r_X(t) \triangleq \frac{f_X(t)}{\bar{F}_X(t)}$, for the *age* t such that $\bar{F}_X(t) > 0$.

We assume that $r_X(t)$ is a real-valued, differentiable function. $r_X(t)$ is said to be increasing failure rate (IFR) when $r_X(t)$ is strictly increasing function in t, i.e., $r'_X(t) > 0, \forall t$. Likewise, $r_X(t)$ is called decreasing failure rate (DFR) if $r'_X(t) < 0, \forall t$. Suppose that a r.v. X follows a Weibull distribution, $F_X(t) = 1 - \exp(-(t/\beta)^\alpha)$. Then, the corresponding failure rate $r_X(t)$ is DFR (resp. IFR) for $0 < \alpha < 1$ (resp. $\alpha > 1$).

Consider a r.v. X with failure rate $r_X(t)$. We say that X has *positive aging* if $r_X(t)$ is IFR. Similarly, X is said to have *negative aging* if $r_X(t)$ is DFR. When $r'_X(t) = 0$, X is said to have *constant aging*. The aging property can be understood by the notion of residual time. Let a r.v. X be a life time and denote the residual time until the end of life X by X_t, when the current age is t (i.e., on the condition that $X \geq t$). Note that X_t is also a random variable, and its complementary CDF (CCDF) is given by $\mathbb{P}[X_t > x] = \mathbb{P}[X - t > x \mid X > t]$. Then, when the failure rate $r_X(t)$ is DFR (or negative aging), the residual time X_t stochastically increases with time t [20]. In case of IFR (or positive aging), X_t stochastically decreases with time t.

To interpret it in our context where X is inter-AP arrival time, on the condition that X is negative aging and a mobile has no contact with an AP until t, the remaining time until encountering an AP from t stochastically increases with t. As the remaining time increases, the sensing interval should accordingly increase to save energy. For the case of IFR, a similar interpretation can be stated. This aging concept has recently been used in [25], which proves that this *memory* structure arises from general mobility patterns and can be used for a better design of mobile wireless networks.

III. Solutions and Algorithm

In this section, we first present the technical challenges of (OPT) by introducing the examples for two types of sensing policies. Then, we provide reasonable approximations of (OPT) and develop a modified objective function that allows mathematical tractability. Then, we derive the conditions for optimality, followed by the practical implications into a good Wi-Fi sensing algorithm.

A. Challenges

1) Homogeneous Poisson Sensing: Let us first consider a simple case when sensing is performed following a homogeneous Poisson process in order to clearly see the tradeoff between energy efficiency and performance as well as to have a taste of challenges residing in our optimization problem. Consider a homogeneous Poisson process with rate μ and an AP contact duration time Y. Suppose Y can be expressed in terms of another positive r.v. A such that $\mathbb{P}[Y > y] = \mathbb{E}_A[\mathrm{e}^{-Ay}]$.[5] Putting $c_\mathrm{s} = \gamma = r_w = 1$, (OPT) can be rearranged as

$$(\mathrm{OPT}) = \min_{\mu} \{\mu \mathbb{E}[X] + \mathbb{E}[\min(Y, S)]\} \tag{2}$$

where S is an exponential r.v. (because of homogenous Poisson sensing), and

$$\begin{aligned}\mathbb{E}[\min(Y,S)] &= \int_0^\infty \mathbb{P}[Y > x]\mathbb{P}[S > x]\mathrm{d}x \\ &= \int_0^\infty e^{-\mu x}\mathbb{E}_A[e^{-Ax}]\mathrm{d}x = \mathbb{E}_A\left[\frac{1}{\mu + A}\right].\end{aligned} \tag{3}$$

Then, it follows from (3) that (2) becomes

$$\min_{\mu}\left\{\mathbb{E}_A\left[\mu\mathbb{E}[X] + \frac{1}{\mu + A}\right]\right\} \tag{4}$$

which clearly shows the tradeoff: As μ increases (i.e., sensing with higher frequency), the energy consumption term $\mu\mathbb{E}[X]$ increases, whereas the contact loss term $1/(\mu + A)$ decreases.

Note that (4) is invariant with respect to the distribution of X except for $\mathbb{E}[X]$, which is due to the restriction of our focus to homogeneous Poisson sensing processes. To put it another way, in order to find a more optimal sensing, it is inevitable that the sensing policy is modeled by a more general stochastic process, i.e., nonhomogeneous Poisson processes, which lends itself to adaptation to distributional properties of X and A, along with $\mathbb{E}[X]$.

2) Deterministic Sensing: We now consider another class of sensing processes: deterministic sensing. Recall that this case can be regarded as nonhomogeneous Poisson processes, where the rate $n(t)$ is a Dirac comb (See Section II-A). Then, it is not hard to see that computing the optimal solution of (OPT) is equivalent to solving the following problem, expressed in terms of distribution $F_X(\,\cdot\,)$ of the inter-AP arrival time X

$$(\mathrm{OPT}) = \min_{(T_k)_{k=0}^\infty} \sum_{k=1}^\infty \int_{T_{k-1}}^{T_k} \{c_\mathrm{s}k + \gamma r_w l(T_k - t)\}\mathrm{d}F_X(t). \tag{5}$$

Yet, solving (5) is significantly challenging due to the following facts.

1) Analytical solutions are hard to obtain because each objective is a function of an infinite sequence $(T_k)_{k=0}^\infty$. On top of that, even for well-known distributions of X, there exists a complex coupling between a nonlinear function $l(\,\cdot\,)$ and the PDF $\mathrm{d}F_X(\,\cdot\,)$ inside the integral.
2) Computing the solutions numerically is also challenging, due to a large search space generated by an infinite number of possible combinations [26].

A similar problem for deterministic sensing processes has been studied in reliability theory, referred to as *inspection problem* [27], only when the contact duration time Y is infinite (w.p. 1). Barlow *et al.* [27] developed a recurrence formula, instead of a fully analytical solution, only in the limited case.[6] It still remains open as to how to solve the problem for general distributions.

[5] In this case, Y is called a completely monotone (CM) distribution. We use a CM distribution only to better illustrate the simplistic form of the tradeoff. Many types of distribution including exponential and Weibull are known to belong to CM class.

[6] When $f_X(t)$ is PF_2 (Pólya frequency function of order 2). As discussed in [28, Remark 2.2], if the failure rate function $r(t)$ is DFR, $f_X(t)$ does not belong to the class of PF_2. Note that DFR X has been largely seen in the real mobility traces (see Section VI for details).

B. Approximations

Obtaining the analytical form of $\mathbb{E}[l(S)] = \mathbb{E}[\mathbb{E}[l(S)|X]]$ entails two key obstacles: 1) the analytical form of S's distribution (conditioned on X), given by

$$\mathbb{P}[S > s \,|\, X = t] = \exp\left(-\int_t^{t+s} n(u)\mathrm{d}u\right) \tag{6}$$

is difficult to compute; and 2) nonlinear loss time function $l(\,\cdot\,)$ is involved there. Thus, to get a tractable form of the objective function, we make two approximations, summarized in what follows.

First, we use an upper bound of $\mathbb{E}[\mathbb{E}[l(S)|X]]$. Note that it is easy to show that $l(s)$ is concave in s, verified by

$$l(s) = \int_0^\infty \mathbb{P}[\min\{Y, s\} > y]\mathrm{d}y = \int_0^s \mathbb{P}[Y > y]\mathrm{d}y \tag{7}$$

whereupon we have $l''(s) = -f_Y(s) < 0$. It follows from Jensen's inequality that $\mathbb{E}[\mathbb{E}[l(S) \,|\, X]] \leq \mathbb{E}[l(\mathbb{E}[S \,|\, X])]$. Manipulating $\mathbb{E}\,[S \,|\, X]$ becomes much more tractable due to the absence of $l(\,\cdot\,)$. Now, for the computation of the new target $\mathbb{E}[l(\mathbb{E}[S \,|\, X])]$, it is required to get the analytical form of $\mathbb{E}[S \,|\, X = t]$ for $t > 0$. However, it is still challenging to compute because an integral with $n(t)$ is an exponent of the function $\exp(\,\cdot\,)$ in (6). To tackle this problem that is of vital importance to the optimization (OPT), we only assume that the following two quantities vary smoothly with k:

$$\mathbb{E}[T_k - T_{k-1}], \quad \sigma^2_{T_k - T_{k-1}}$$

for $k \geq 1$, where the second term is the variance of $T_k - T_{k-1}$. This assumption implies that when a mobile conducts sensing, the average and variance of the next sensing time should be slowly varying with each sensing. It should be remarked that the assumption specifies nothing else but the tendency of the first two moments, so that $n(t)$ is still allowed to vary with time t. Recall that our target is to compute $\mathbb{E}\,[S \,|\, X = t]$, where $S = T(t) - t$ and $T(t)$ is the next sensing time at t, i.e., $T(t) \triangleq \min_k\{T_k \,|\, T_k > t\}$. To simplify exposition, we first adopt

$$I(t) \triangleq T_k - T_{k-1}, \quad \text{such that } T_k > t \geq T_{k-1}.$$

The practical value of this *slowly varying* moment assumption lies in that it enables us to get a manipulative form of $\mathbb{E}[S \,|\, X = t]$, which is the mean residual time of a point process at arbitrary time t. Note the *arbitrary* time t is more likely to fall in larger sensing intervals around t. Thus, it follows from the Palm inversion formula [29, Theorem 7.3.1]

$$\Lambda(t) \triangleq \mathbb{E}[S \,|\, X = t] = \frac{1}{2}\left(\mathbb{E}[I(t)] + \frac{\sigma^2_{I(t)}}{\mathbb{E}[I(t)]}\right) \tag{8}$$

also known as Feller's paradox. To summarize, $\mathbb{E}[l(\mathbb{E}[S \,|\, X])]$ can be further approximated when the first two moments of intersensing times do not vary much with each sensing event.

Approximating the original contact loss time $\mathbb{E}[l(S)]$ with $\mathbb{E}[l(\mathbb{E}[S \,|\, X])]$, and plugging (8) into (OPT), and the original optimization objective can be rearranged as

$$\begin{aligned}
&\min_{(n(t))_{t=0}^\infty} c_{\mathrm{s}}\mathbb{E}\left[\int_0^X n(\tau)\mathrm{d}\tau\right] + \gamma r_w \mathbb{E}\left[l\left(\Lambda(X)\right)\right] \\
&= \min_{(n(t))_{t=0}^\infty} \int_0^\infty \left\{c_{\mathrm{s}}\int_0^t n(\tau)\mathrm{d}\tau f_X(t) + \gamma r_w l(\Lambda(t)) f_X(t)\right\}\mathrm{d}t \\
&= \min_{(n(t))_{t=0}^\infty} \int_0^\infty c_{\mathrm{s}} n(t)\bar{F}_X(t) + \gamma r_w l(\Lambda(t)) f_X(t)\mathrm{d}t
\end{aligned} \tag{9}$$

where $f_X(\,\cdot\,)$ is the density function of the inter-AP arrivals.

Here, we can see that the first term inside the integral of (9) is still a function of $n(t)$, which can be further simplified from the fact that replacing the *instantaneous* rate $n(t)$ with its *short-term average* rate $1/\mathbb{E}[I(t)]$ does not make significant difference to (9) if $\bar{F}_X(t)$ inside its integral is a well-defined smooth function. Finally, we present the modified objective approximating the original optimization objective, expressed by X, $1/\mathbb{E}[I(t)]$, and $\sigma^2_{I(t)}$:

$$\min_{(I(t))_{t=0}^\infty} \int_0^\infty \frac{c_{\mathrm{s}}}{\mathbb{E}[I(t)]}\bar{F}_X(t) + \gamma r_w l(\Lambda(t)) f_X(t)\mathrm{d}t. \tag{xOPT}$$

C. Optimality Conditions

The optimal sensing sequence from (xOPT) is computed by controlling the following two items: 1) the expectation $\mathbb{E}\,[I(t)]$, and 2) the variance $\sigma^2_{I(t)}$. Since the mean $\mathbb{E}[I(t)]$ and the variance $\sigma^2_{I(t)}$ are independent, we can freely adjust the variance while keeping the same mean of intersensing time. Note that for a fixed $\mathbb{E}[I(t)]$, (xOPT) increases with $\sigma^2_{I(t)}$ because the loss function $l(\Lambda(t))$ increases with $\Lambda(t)$. Thus, given $\mathbb{E}[I(t)]$, we first search the space of the sensing process $n(t)$ that minimizes the variance. It is not hard to see that a *deterministic* sensing process achieves the smallest variance, which is zero. This observation further simplifies the optimization (xOPT), where it suffices to solve (xOPT) over the space of deterministic sequences of sensing intervals with rate $n(t)$. Putting $\sigma^2_{I(t)} = 0$, $\Lambda(t)$ in (8) becomes $\mathbb{E}[I(t)]/2$. The objective function is then expressed as a functional $A[I]$

$$A[I] \triangleq \int_0^\infty \left\{\frac{c_{\mathrm{s}}}{I(t)}\bar{F}_X(t) + \gamma r_w l\left(\frac{I(t)}{2}\right) f_X(t)\right\}\mathrm{d}t. \tag{10}$$

Note here that we need to determine only $\mathbb{E}[I(t)] = I(t)$ ($I(t)$: the length of sensing interval containing t) where the the equality holds because $I(t)$ is *no longer* random. To put it another way, we have now demonstrated that optimal Wi-Fi sensing algorithms should be *deterministic*. As compared to (5), the deterministic formulation (10) has been properly justified and, thanks to its simplistic integral form, it is *amenable* to functional analysis that is applied to yield the following theorem. We apply the calculus of variations [30] to $A[I]$ with the objective of finding an optimal $I(t)$, which leads to Theorem 1 presenting necessary and sufficient conditions for optimality. Denote by $(I^\star(t))_{t=0}^\infty$ an optimal sensing interval function that minimizes $A[I]$.

Theorem 1 (Optimality Condition):

i) *Necessity*: (Recall that $r_X(t)$ is the failure rate of X.)

$$(I^\star(t))^2 \overline{F}_Y\left(\frac{I^\star(t)}{2}\right) = \frac{2c_{\mathrm{s}}}{\gamma r_w r_X(t)}. \tag{11}$$

ii) *Sufficiency*: (11) is also sufficient under the following condition:

$$\overline{F}_Y\left(\frac{I^\star(t)}{2}\right) > \frac{I^\star(t)}{4} f_Y\left(\frac{I^\star(t)}{2}\right). \quad (12)$$

The proof is presented in the Appendix. As expected, Theorem 1 states that the optimal sensing sequence $I^\star(t)$ highly depends on the distributions of both inter-AP arrival and contact duration times, X and Y. In Section III-D, we will explain that the sufficient condition in (12) is highly likely to be satisfied in practice, implying that the condition (11) is nearly necessary and sufficient for optimality. This motivates us to propose a novel sensing algorithm driven by (11) in Section III-C.

D. Mildness of Sufficient Condition (12)

Now, we investigate the sufficiency region of the sensing interval $I(t)$. Since the sufficient condition (12) depends only on the distribution of contact duration time Y, we divide into four representative cases in terms of the distribution of Y. Throughout this section, we denote by $r_Y(t)$ the failure rate of the contact duration time Y, hence the sufficient condition (12) can be rewritten as $\frac{4}{I(t)} - r_Y(\frac{I(t)}{2}) > 0$, where $r_Y(t) = f_Y(t)/\bar{F}_Y(t)$. For notational simplicity, we drop the superscript $\star$ in $I^\star(t)$ in the rest of this section, unless confusion arises.

a) Heavy-Tailed Y in Generalized Pareto: When Y follows a Generalized Pareto distribution with heavy-tail, we have $\mathbb{P}[Y > y] \sim (1 + \frac{\xi y}{\sigma})^{-\frac{1}{\xi}}$ with a shape parameter $\xi > \frac{1}{2}$ and a scale parameter $\sigma > 0$. The term $\frac{4}{I(t)} - r_Y(\frac{I(t)}{2})$ is always positive since $r_Y(\frac{I(t)}{2}) = \frac{2/\xi}{2\sigma/\xi + I(t)}$ is always less than $\frac{4}{I(t)}$, meaning that the interval sequence always be within the sufficiency region over time t. Note that the actual lengths of the increasing intervals can be numerically computed by solving the optimality condition (11) for the given distribution of inter-AP arrival time X and contact duration time Y.

b) Not Heavy-Tailed Y in Generalized Pareto: When Y is Generalized Pareto r.v and not heavy-tailed, we have $\mathbb{P}[Y > y] \sim (1 + \frac{\xi y}{\sigma})^{-\frac{1}{\xi}}$ with $\xi < \frac{1}{2}, \sigma > 0$. Then, (12) becomes

$$\frac{4}{I(t)} - \frac{1}{\sigma + \frac{\xi I(t)}{2}} > 0 \Leftrightarrow I(t) < \frac{4\sigma}{1-2\xi} = \frac{4\mathbb{E}[Y](1-\xi)}{1-2\xi}.$$

Shape parameter ξ's measured from our trace in Section VI-B are greater than -0.5, meaning that the intervals satisfy the sufficient condition when $I(t) < \zeta \mathbb{E}[Y]$, $\zeta \in (3, \infty)$.

c) Weibull Y: When Y follows a Weibull distribution, we have $\mathbb{P}[Y > y] = \exp\{-(y/\mu)^\beta\}$. For a Weibull distribution with the shape parameter β and the scale parameter μ, the condition for increasing interval is given by

$$\frac{4}{I(t)} - \frac{\beta I(t)^{\beta-1}}{\mu^\beta 2^{\beta-1}} > 0 \Leftrightarrow I(t) < \frac{2^{1+1/\beta}\mu}{\beta^{1/\beta}} = \frac{2^{1+1/\beta}\mathbb{E}[Y]}{\beta^{1/\beta}\Gamma(1+1/\beta)} \quad (13)$$

The βs of Y from our trace range over the interval [0.3, 2]. By rewriting (13) for such a range of β, the sufficiency interval region is $I(t) < \zeta\mathbb{E}[Y]$, $\zeta \in [2.25, 120]$.

d) Exponential Y: Note that a Weibull r.v. with $\beta = 1$ is exponential. Thus, the condition for increasing intervals follows from (13), given by: $I(t) < 4\mathbb{E}[Y]$. This again means that the optimality holds unless the sensing interval exceeds $4\mathbb{E}[Y]$.

The sufficiency condition (12) states that the optimal sensing intervals are not significantly large, compared to the AP contact duration time Y, whose mildness can be checked by measuring the distribution of Y from real traces. According to our measurement, the optimal sensing interval is highly likely within the sufficiency region because: 1) the penalty term from the contact loss in our optimization problem makes the interval scale smaller compared to $\mathbb{E}[Y]$, and 2) measured $\mathbb{E}[Y]$ is more than 2 times of measured $\mathbb{E}[X]$ [2].

E. Increase/Decrease of Optimal Sensing Interval

We now present the increase/decrease of optimal sensing intervals in relation to the notion of aging of the inter-AP arrival time X. To that end, consider three cases when X is negative, constant, and positive aging (i.e., $r'(t) < 0, = 0, > 0$, respectively). The trends are summarized as follows: *Optimal sensing intervals $I(t)$ should increase, be periodic, and decrease if the distribution of X has negative, constant, and positive aging, respectively,* as stated in Table I in Section I.

To understand why, by rearranging the optimality condition (11) with $r_X(t)$ and $r_Y(t)$, we get

$$I(t)^2 \exp\left(-\int_0^{I(t)/2} r_Y(x)dx\right) = \frac{2c_s}{\gamma r_w r_X(t)}. \quad (14)$$

Taking log on both sides of (14) and differentiating w.r.t. t, we have the following:

$$\frac{I'(t)}{2}\left\{\frac{4}{I(t)} - r_Y\left(\frac{I(t)}{2}\right)\right\} = -\frac{r'_X(t)}{r_X(t)}. \quad (15)$$

Once the failure rates of X and Y are given, (15) enlightens us upon the sign of $I'(t)$. This further generates the conditions for the signs of $I'(t)$ and $\frac{4}{I(t)} - r_Y(\frac{I(t)}{2})$, which provide the information on when the sensing intervals should increase or decrease, as elaborated upon shortly. We can easily check that $r_X(t) > 0$ and the sufficient condition in (12) is exactly equal to $\frac{4}{I(t)} - r_Y(\frac{I(t)}{2}) > 0$ in (15). Therefore, whether optimal sensing intervals should increase or decrease upon the failure of detecting an AP (i.e., the sign of $I'(t)$) depends only on the sign of $r'_X(t)$, which directly represents the aging property of inter-AP arrival time X. When X has constant aging (i.e., $r_X(t) = c$ for some constant c, and hence is memoryless), $I(t)$ becomes constant over time as well, which in turn implies that the optimal sensing process should be periodic.

IV. Optimality on a Different Objective

We have so far studied the optimal sensing interval for minimizing the scanning energy penalized by contact loss in (OPT), and showed that the increase/decrease of the optimal sensing interval only depends on aging of inter-AP arrival time. However,

it still remains unclear whether such dependency between optimality and aging holds for other types of objectives. Thus, in this section, to strengthen our engineering insight on increase/decrease of sensing interval, we further investigate the connection between optimality of sensing interval and aging of inter-AP arrival time under a different type of objective, sensing energy per a transmission bit, which was also handled in [13].

A. Objective

We consider the problem of minimizing the average sensing energy per unit amount of data transmitted over Wi-Fi APs.

OPT2: Minimize average sensing power per bits

$$\min_{(n(t))_{t=1}^{\infty}} \frac{c_{\mathrm{s}}\mathbb{E}[N(X)]}{r_w\mathbb{E}[g(S)]} \tag{OPT2}$$

where $g(S)$ is the remaining contact duration after AP detection (i.e., $g(S) = Y - l(S)$).

B. Approximation

As mentioned in Section III-B, obtaining the analytical form of $\mathbb{E}[g(S)]$ is hard due to difficulty of computing the distribution of S and nonlinear function of $g(\cdot)$. Thus, (OPT2) is also hard to be directly analyzed, and hence needs to be approximated. To handle this, we again use Jensen's inequality to approximate $\mathbb{E}[g(S)]$ to $\mathbb{E}[g(\mathbb{E}[S])]$. Then, we assume slowly varying sensing intervals to use Feller's paradox in (8). The approximated form of (OPT2) is as follows:

$$\min_{(n(t))_{t=0}^{\infty}} \frac{c_{\mathrm{s}}\mathbb{E}\left[\int_0^X n(\tau)\mathrm{d}\tau\right]}{r_w\mathbb{E}[g(\Lambda(X))]} = \min_{(n(t))_{t=0}^{\infty}} \frac{\int_0^{\infty} c_{\mathrm{s}} n(t)\bar{F}_X(t)\mathrm{d}t}{\int_0^{\infty} r_w g(\Lambda(t)) f_X(t)\mathrm{d}t}. \tag{xOPT2}$$

Recall that $\Lambda(t) = \frac{1}{2}\left(\mathbb{E}[I(t)] + \frac{\sigma^2_{I(t)}}{\mathbb{E}[I(t)]}\right)$. We now focus our attention on the objective function in (xOPT2). Since the function g is nonincreasing, the variance of sensing interval $\sigma^2_{I(t)}$ should be zero to minimize (xOPT2), which means that the sensing interval should be deterministic. If $\bar{F}_X(t)$ is a well-defined smooth function, we can replace the rate function $n(t)$ by the interval $I(t)$ without significant difference to (xOPT2). Note that such approximation technique is similar to that of (10) in Section III-B

$$A'[I] \triangleq \frac{\int_0^{\infty} \frac{c_{\mathrm{s}}}{I(t)}\bar{F}_X(t)\mathrm{d}t}{\int_0^{\infty} r_w g\left(\frac{I(t)}{2}\right) f_X(t)\mathrm{d}t}. \tag{16}$$

C. Necessary Condition for the Optimal Sensing Interval

We apply the calculus of variations [30] to find an optimal sensing interval $I^\star(t)$ for (xOPT2). The main challenge for this optimization is that the form of the objective in (xOPT2) is a fraction of functionals, which was not handled in Section III. In the following theorem, we address this challenge and show the necessary condition of the optimal sensing interval $I^\star(t)$ with respect to (xOPT2).

Theorem 2 (Necessary Condition): The optimal sensing interval $I^\star(t)$ in (xOPT2) holds the following necessary condition:

$$(I^\star(t))^2\overline{F}_Y\left(\frac{I^\star(t)}{2}\right) = \frac{2B}{r_X(t)} \tag{17}$$

where $r_X(t)$ is a failure rate of AP interarrival time X, and $B = \frac{\int_0^{\infty} g(I^\star(t)/2) f_X(t)\mathrm{d}t}{\int_0^{\infty} \bar{F}_X(t)/I^\star(t)\mathrm{d}t}$.

The proof is presented in the Appendix. It is rather surprising that the necessary condition for (xOPT2) in Theorem 2 is identical to that for (xOPT) in Theorem 1 except the unknown variable B. At the same time, this similarity gives us one fundamental illumination: The optimal sensing interval $I^\star(t)$ shares the common *aging* properties summarized in Table I, whereas the two corresponding optimal solutions can take vastly different forms depending on the distribution of Y [due to the second factor in the left-hand sides of (11) and (17)]. To corroborate this illumination, by rearranging the optimality condition (17) with proportionality constant $2B$, we get

$$I(t)^2 \exp\left(-\int_0^{I(t)/2} r_Y(x)dx\right) = \frac{2B}{r_X(t)}. \tag{18}$$

Then, we can take logarithm on both sides of (18) and differentiate w.r.t. t, which yields the following:

$$\frac{I'(t)}{2}\left\{\frac{4}{I(t)} - r_Y\left(\frac{I(t)}{2}\right)\right\} = -\frac{r'_X(t)}{r_X(t)}. \tag{19}$$

Since we have already shown that the condition $\frac{4}{I(t)} - r_Y(\frac{I(t)}{2}) > 0$ can be easily satisfied in Section III-D, whether optimal sensing intervals should increase or decrease upon the failure of detecting an AP (i.e., the sign of $I'(t)$) depends only on the sign of $r'_X(t)$ that represents the aging property of inter-AP arrival time X. Thus, the optimal sensing interval for (xOPT2) also has the common aging property summarized in Table I.

While our finding holds only for a certain form of optimization problems formulated in terms of sensing energy and contact duration, it clearly delineates the overall correlation structure between two distributions, i.e., sensing interval and inter-AP arrival time. This finding also opens up new potential possibilities for a variety of heuristic algorithms capitalizing on the correlation structure.

V. WiSAG: Theory-Inspired Sensing Algorithm

We now develop a Wi-Fi sensing algorithm, called *WiSAG* (Wi-fi Sensing with AGing), motivated and inspired by analytical findings in Theorems 1 and 2. The algorithm can be oriented toward objective (OPT) and (OPT2) by adopting the (11) and (17), respectively.

WiSAG (Wi-fi Sensing with AGing)

Preprocessing: A mobile computes a sensing interval function $I(t)$ according to (11) or (17) depending on the objective. The computation is based on inputs of the distributions of inter-AP arrival and contact duration, $F_X(\cdot)$ and $F_Y(\cdot)$.

At each phase p:

1. *Initialization*.

Set $T_0 = 0$, and $T_1 = I(T_0)$.
Set the clock $t = 0$ and the counter $k = 1$, and run the clock.
2. **If** $t == T_k$,
Sense Wi-Fi
If no AP is sensed and associated,
Set $T_{k+1} = T_k + I(T_k)$ and $k = k + 1$
Else communicate with the associated AP until the AP connection is lost and then end the phase p
End If
End If

A few remarks are in order. First, we assume that the distributions of X and Y are given to a user. This requires a mobile user to have a reasonable amount of training time. Although the detailed algorithm for training is beyond the scope of this paper, we can employ the training methods for other similar statistics, e.g., visiting patterns to a specific location such as office or home, used in other research [21], [22]. Second, a practical algorithm like WiSAG is unable to know whether the user misses an AP due to fast mobility or not, which differs from the model used in the analysis. In such a case, in the model, a new phase is assumed to start, yet in practice, the user is still in the old phase and keeps increasing (or decreasing) the sensing intervals. We later show that Section VI demonstrates that such a difference is minor.

Computation of (17): To compute $I(t)$ from (17), we should compute B, which can be computationally challenging because the numerator and denominator of B are functionals of $I(t)$, which hinder finding the closed form of $I(t)$. We further develop a heuristic approach to address such infeasibility in computing (17). The mathematical trick for circumventing direct computation of B lies in realizing the very fact that $r_w B/c_\mathrm{s}$ is the reciprocal of the cost of (OPT2) with the interval $I(t)$. That is, if sensing with $I(t)$ computed with a certain constant B leads to the cost which *coincides* with $c_\mathrm{s}/r_w B$, $I(t)$ inadvertently happens to satisfy the necessary condition. By exploiting this idea, we propose an iterative algorithm for finding $I(t)$ for (OPT2). At each iteration, in order to get the cost of WiSAG with the interval $I(t)$, we run a multitude of numerical simulations where the parameters of the scenario are fitted from training data and calculate the average cost. This iteration ends when the convergence of B is diagnosed or the iteration count exceeds a certain threshold.

Approximation of $I(t)$ in (17)

Initialization. Mobiles learn the distributions of inter-AP arrival and contact duration, $F_X(\cdot)$ and $F_Y(\cdot)$ and their expectation $\mathbb{E}[X]$ and $\mathbb{E}[Y]$. They also decide the parameter m, d, ϵ, and set $B(0) = \frac{\mathbb{E}[Y]^2}{\mathbb{E}[X]+\mathbb{E}[Y]}$.
At each iteration i,
1. Compute the interval $I(t)$ using the following equation:

$$I(t)^2 \overline{F}_Y\left(\frac{I(t)}{2}\right) = \frac{2}{r_X(t)} B(i-1). \tag{20}$$

2. Run WiSAG with $I(t)$ for m times in numerical simulations, and set $B(i)$ as follows:

$$B(i) = \frac{1}{m}\sum_{j=1}^{m} \frac{C_j}{N_j} \tag{21}$$

where N_j and C_j are the number of sensings and contact duration captured by WiSAG at jth simulation.
3. Repeat steps 1 and 2 until $|B(i) - B(i-1)| < \epsilon$ or $i > d$.

VI. Trace-Driven Evaluation

A. Dataset

We use Wi-Fi AP contact logs of 84 iPhone 3G/3GS users and 63 Android users in the KAIST campus. In case of iPhone measurement, users downloaded a measurement application and tested it for about 18 days in February 2010, recruited from a Korean iPhone user community. The measurement application runs in the background to record Wi-Fi AP encounters every 3 min. The granularity of 3 min may lose an event with finer granularity, e.g., handoff. The choice of 3 min is made to slow down the speed of consuming battery. We further measure the Wi-Fi contact logs of KAIST campus students for 14 days. We recruit 60 students with Android smartphones and let them download a measurement application that logs Wi-Fi contacts with the granularity of 1 min. In both measurements, the captured Wi-Fi APs include both private APs and commercial APs. The log files are periodically uploaded to a log-server over ftp connections. In addition, we also consider active hour (AH) scenarios of both traces, i.e., the traces from 9:00 to 23:00, because, in practice, many users may carry the mobile devices during active hours and charge them at night.

B. Individual Aging Patterns

We started with searching for distributions that fit best IAT and CDT of each individual. We selected three candidates of Weibull, Exponential, and Generalized Pareto because: 1) Weibull and Exponential distributions [2], [13] are reported to follow IAT and/or CDT in literature; and 2) Generalized Pareto significantly differs from Weibull and Exponential, possessing a power tail. We use a Cramer–Smirnov–Von–Mises (CSVM) statistical hypothesis test [31], [32], which is popularly used to find a best fit. A CSVM test rejects a tested distribution when its CSVM statistic value is less than the Critical Values determined by a significance level. We test it with a popular significance level 0.1 and summarize the result of CSVM test in Table II. Each element in Table II consists of: 1) % of accepted users, along with 2) % of users that have the best match with the corresponding distribution, which is in parentheses. We refer the readers to [31] and [32] for the details of CSVM. Table II tells us that most users' IAT and CDT distributions follow Weibull or Generalized Pareto (Gen. Pareto), where Generalized Pareto's portion is larger.

It now remains to figure out the parameters of each distribution, i.e., α in Weibull and ξ in Generalized Pareto, which shows the aging property of IAT and CDT. The actual value of α and ξ for each individual will also be used in determining the actual sensing intervals of WiSAG. In Fig. 2(a) [resp. (b)],

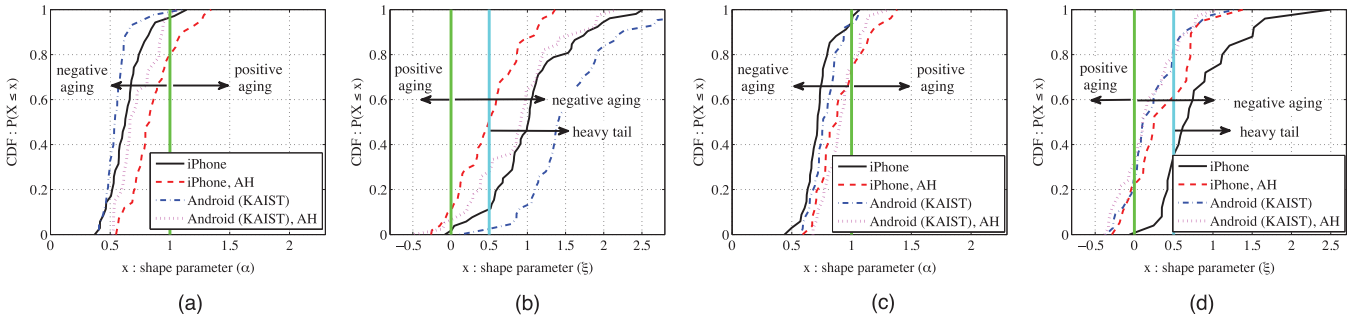

Fig. 2. *Distribution of shape parameter α and ξ in IAT and CDT of each individual in the traces*. (a), (b) CDFs of parameter α and ξ of IAT distributions of users identified as experiencing Weibull and Generalized Pareto IATs. (c), (d) CDFs of parameter α and ξ of CDT distributions of users identified as having Weibull and Generalized Pareto CDTs.

TABLE II
CSVM TESTS FOR THE DATASETS WITH SIGNIFICANCE LEVEL $= 0.1$. EACH ELEMENT=% OF ACCEPTED USERS (% OF USERS WITH THE BEST MATCH)

	Weibull	*Gen. Pareto*	*Exp.*
IAT: iPhone	42 (20)	64 (80)	7 (0)
IAT: KAIST	55 (45)	70 (54)	10 (1)
IAT: iPhone(AH)	54 (18)	68 (79)	22 (3)
IAT: KAIST(AH)	65 (28)	73 (69)	40 (3)
CDT: iPhone	48 (28)	52 (68)	13 (4)
CDT: KAIST	64 (42)	56 (53)	30 (5)
CDT: iPhone(AH)	40 (30)	40 (66)	23 (4)
CDT: KAIST(AH)	68 (32)	67 (60)	43 (8)

we plot the CDF of α for the users that experience a Weibull (resp. ξ for Pareto) IAT distribution, demonstrating that about 94% of overall users go through negative aging in their IAT distributions, i.e., $\alpha < 1$ or $\xi > 0$. We also plot the CDF of IATs during AH, which also shows that 85% users have negative aging IAT distributions. Remarkably, all students in KAIST traces are perceived to undergo negative aging and most of them show heavy-tail distributions. However, when we focus on their IAT distributions during AH, 8% of students in KAIST appear to have positive aging. For the case of CDT distribution, the CDFs of α and ξ are shown in Fig. 2(c) and (d). The shape parameter α of Weibull-fitted users ranges from 0.3 and 1.5, and ξ of Pareto-fitted users are greater than -0.5. These results support the fact that the sufficient condition (17) for the optimality can be highly likely to be satisfied (see Section III-D).

The key message of our measurement-based analysis here is that a large portion of users experience negative aging, thereby implying that the sensing algorithms that increase the sensing intervals, such as AI [18], ExBackoff [33], and also WiSAG, take the right direction. However, just increasing intervals is not sufficient to guarantee high performance: The simple patterns of increasing intervals, such as linear in AI or exponential in ExBackoff, do not always perform very well, and we need to adaptively control the sensing intervals like WiSAG that actively exploit the diverse *failure rates* of IAT over time. Furthermore, the appearance of positive aging users during active hours indicates that, in some cases, algorithms with increasing interval, such as AI and ExBackoff, can perform poorly, whereas WiSAG can easily adapt to the user pattern with the decreasing sensing interval. We now verify such a reasoning through the trace-driven simulations.

TABLE III
SENSING INTERVAL (IN THE UNIT OF SECONDS) USED IN EACH ALGORITHM. THE SENSING INTERVALS FOR AI AND EXBACKOFF ARE GIVEN IN TERMS OF INDEX k, WHICH STANDS FOR THE kTH SENSING ATTEMPT (AI: INCREMENT$\times k$, EXBACKOFF: CONSTANT$\cdot$BASE^k)

	objectives	iPhone	KAIST	*iPhone(AH)*	*KAIST(AH)*
PERD	(OPT) w/ γ=0.05	376	678	369	381
	(OPT) w/ γ=0.3	223	291	143	155
	(OPT2)	12200	11400	2700	4880
AI	(OPT) w/ γ=0.05	$56{\cdot}k$	$63{\cdot}k$	$52{\cdot}k$	$34{\cdot}k$
	(OPT) w/ γ=0.3	$9{\cdot}k$	$8{\cdot}k$	$8{\cdot}k$	$4{\cdot}k$
	(OPT2)	3707	1860	410	740
ExBackoff	(OPT) w/ γ=0.05	$37{\cdot}1.17^k$	$71{\cdot}1.13^k$	$36{\cdot}1.15^k$	$37{\cdot}1.13^k$
	(OPT) w/ γ=0.3	$22{\cdot}1.03^k$	$29{\cdot}1.03^k$	$14{\cdot}1.05^k$	$15{\cdot}1.03^k$
	(OPT2)	$2600{\cdot}2.62^k$	$1140{\cdot}2.72^k$	$270{\cdot}1.92^k$	$488{\cdot}2.82^k$

C. Tested Algorithms

We test three sensing algorithms in literature: **PERD** (Periodic) [13], [18], which senses APs over fixed periodic intervals; **AI** (Additive Increase) [18], which increases the sensing interval by a fixed increment after each sensing; and finally **ExBackoff** (exponential backoff) [33], which exponentially increases the sensing interval. Each algorithm has a parameter such as the period in PERD, the increment in AI, and the constant and base in ExBackoff. In our comparison of the performance, we use the "best" version of each algorithm in the sense that the *best* parameter (which shows the minimum penalized cost) is searched by running the corresponding algorithm offline multiple times over a large number of parameter choices. Table III summarizes the sensing intervals of the compared algorithms whose parameters are fitted for (OPT) with γ and (OPT2). From Table III, we can observe a dependency between the resulting sensing intervals and the penalty weight for Wi-Fi contact loss γ: The length of sensing interval is *negatively* correlated with γ. As γ increases, each algorithm tends to reduce the WiFi contact loss more aggressively, thereby shortening their sensing intervals. This means that the value of γ can be viewed as a flexible knob representing the application-specific tradeoff between sensing interval and Wi-Fi contact loss. In addition, we add one more algorithm, **IDEAL**. Recall that a practical algorithm like WiSAG is unable to know whether the user misses an AP due to fast mobility or not. An omnipotent algorithm "IDEAL" with the optimal sensing intervals can detect such AP missing events and initiate its sensing interval at the start of every phase (see the end of Section V for the discussion).

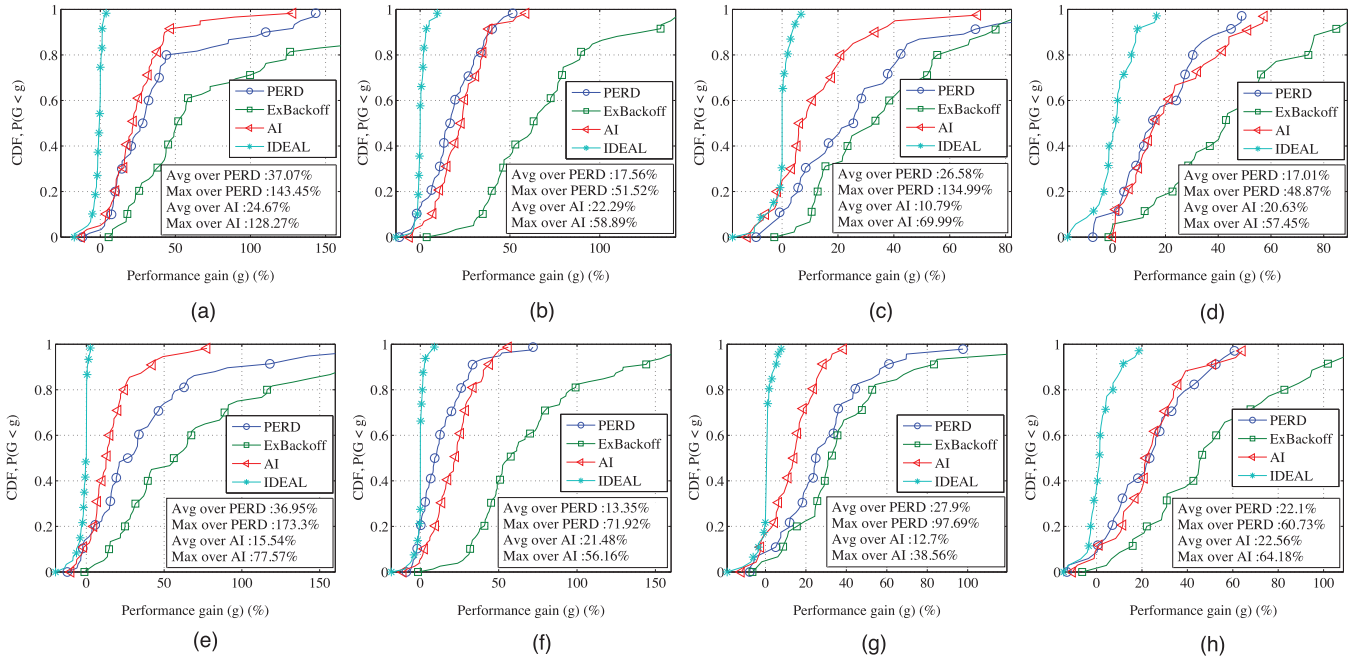

Fig. 3. *Trace-driven comparison of the algorithms for* (OPT) for $c_s = 5J$ and $r_w = 1$ MB/s. The CDF of performance gains experienced by all users are plotted in each scenario. The average gain and maximum gain among all users are marked. (a) 84 iPhone users, $\gamma = 0.05$. (b) 84 iPhone users during AH, $\gamma = 0.05$. (c) 60 KAIST students (using Android smartphones), $\gamma = 0.05$. (d) 60 KAIST students during active hours (using Android smartphones), $\gamma = 0.05$. (e) 84 iPhone users, $\gamma = 0.3$. (f) 84 iPhone users during AH, $\gamma = 0.3$. (g) 60 KAIST students (using Android smartphones), $\gamma = 0.3$. (h) 60 KAIST students during active hours (using Android smartphones), $\gamma = 0.3$.

D. Results

We conduct trace-driven simulations based on the iPhone, KAIST campus traces. In our simulation, each individual mobile runs WiSAG with its own IAT and CDT distributions. Throughout this section, to avoid the confusion between WiSAG for (OPT) and (OPT2), we simply call WiSAG for (OPT) as WiSAG. By referring to previous experimental measurements on the energy consumption and throughput of Wi-Fi [12], [16], we assume that a mobile consumes $5J$ per Wi-Fi sensing and an average throughput is 1 MB/s.

In Fig. 3, we plot the CDF of performance gains experienced by all users in each scenario against four algorithms with respect to (OPT). We test them for two penalty weights $(\gamma = 0.05, 0.3)$. The performance gain over an algorithm 'A' is defined as the increase of the penalized cost (in (OPT)) of 'A' over that of WiSAG, $(\frac{\text{cost of 'A'} - \text{cost of WiSAG}}{\text{cost of WiSAG}} \times 100)$. Fig. 3(a) shows that the average gains of iPhone users over PERD (resp. AI) is 37% (resp. 24%). The maximum gain among all users is 143% over PERD and 128% over AI. In the scenario of Fig. 3(b) where users carry their devices during active hours and charge them at night, WiSAG still outperforms other algorithm by 17% over PERD and 22.3% over AI on average. The maximum gain over PERD (resp. AI) is 51% (resp. 58%). The average performance gap between WiSAG and IDEAL is less than 1.7%, which means that missing AP event due to fast mobility does not have a huge effect on the performance. The average gains over ExBackoff for all cases are more than 65%. Recall that PERD, AI, and ExBackoff operate with the best parameters in terms of our objective, acquired from offline computations over a large set of parameter candidates, whereas WiSAG computes the sensing intervals without any parameter tuning, relying only on the IAT and CDT distributions.

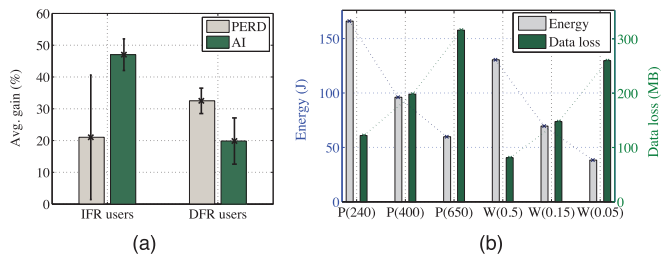

Fig. 4. (a) Average performance gain of IFR (positive aging) and DFR (negative aging) users from both iPhone and KAIST traces during active hours. (b) Tradeoff between the energy and data loss per Wi-Fi contact in KAIST campus trace. In the x-axis, $P(s)$ and $W(r)$ mean periodic sensing with fixed sensing interval s (seconds) and WiSAG with $\gamma = r$, respectively.

As shown in Fig. 3(c) of KAIST users, WiSAG outperforms PERD by 26.5% and AI by 10.8% on average. The maximum gain among all users is 134.7% over PERD and 69.9% over AI. A larger fraction of users with small α in Weibull and large ξ in Pareto (thus negative aging), plotted in Fig. 2(a) and (b), leads to the worse performance in PERD and relatively better performance in AI. However, the active-hour scenario causes the poor performance of AI as shown in Fig. 3(d), where the average gain over PERD (resp. AI) is 17% (resp. 20%). The maximum gains among all users during active hours are 48% over PERD and 57% over AI. We also observe as for such a campus-wide trace that WiSAG performs closely to IDEAL and outperforms ExBackoff more than 60% on average. In the scenarios of Fig. 3(e)–(h), we repeat the evaluation for the penalty weight $\gamma = 0.3$, where the contact loss becomes more weighty. Since WiSAG computes its sensing interval in conformance to the given penalty weight γ, WiSAG still outperforms the existing algorithms with comparable gains to the case of $\gamma = 0.05$. Also, we again observe that PERD performs better than AI for

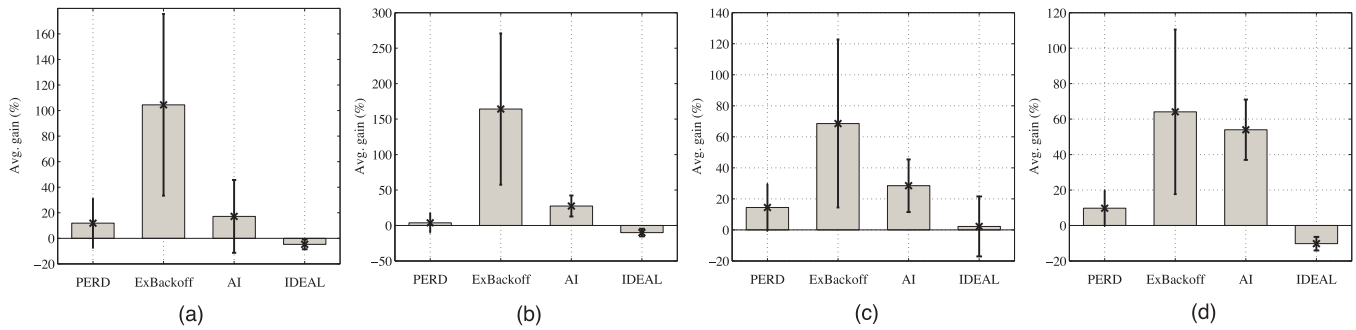

Fig. 5. Gain of WiSAG for (OPT2) for the tested algorithms (PERD, ExBackoff, AI, and IDEAL). (a) iPhone. (b) iPhone (AH). (c) KAIST. (d) KAIST (AH).

both traces and AI performs worse than PERD for active hour traces.

The main reason behind the lower performance of AI during the active hours in both traces is that their shape parameters of IAT distributions tend to form light tails than those during all times, as already observed in Fig. 2(a) and (b). Moreover, due to the increase of the users with positive aging in their IAT distributions, the algorithms with increasing intervals (e.g., AI, ExBackoff) do not work well. To see this, we plot the average gain for IFR (positive aging) and DFR (negative aging) users in Fig. 4. Using a CSVM test on two traces, we pick: 1) IFR users whose IAT distributions during active hours are accepted to Weibull with $\alpha > 1$ or Pareto with $\xi < 0$, and 2) DFR users who are fitted to Weibull with $\alpha < 0.8$ or Pareto with $\xi > 0$. For IFR users, WiSAG outperforms AI by 47% on average since WiSAG successfully reduces the sensing intervals by adapting to the IFR distributions. For DFR users where the optimal sensing interval should increase over time, AI performs better than PERD. However, WiSAG still outperforms AI by 20% because the increasing intervals in WiSAG are more accurate. In Fig. 4(b), we show that the tradeoff between energy and data loss in WiSAG can be controlled by γ. We observe that controlling the balance between the energy and data loss in periodic sensing is conducted on much higher cost region of both energy and data loss than WiSAG.

We also test the heuristic version of WiSAG tailored for (OPT2) based on the heuristic computation of $I(t)$. In Fig. 5, we plot the gain of WiSAG for (OPT2) against the tested algorithms with 95% confidence interval in four traces. To select parameters of the compared algorithms, we test a set of feasible parameters through multiple numerical simulations and pick the one that shows the best average performance in the numerical simulations. Expectedly, it turns out that, in all traces, WiSAG for (OPT2) outperforms the other algorithms, PERD, ExBackoff, and AI. The gain against PERD and AI is 5%–16% and 17%–50%, respectively. These positive gains over the algorithms in comparison validate that proposed WiSAG for (OPT2) performs well on average. However, in some cases, the confidence interval may extend to the negative values, which means that WiSAG for (OPT2) can perform worse for a few users. This is mainly because: 1) the convergence of the algorithm for computing sensing interval is not guaranteed; 2) the algorithm can be trapped into a local optimum. Note also that it is not difficult to design a more sophisticated algorithm avoiding these entrapments, which is beyond the scope of the paper.

VII. Concluding Remarks

The main contributions of this paper are twofold. First, we analyze the fundamental interconnection between the tendency of "best" sensing intervals and distributions of inter-AP arrival and contact duration times. We classify these distributions by aging and show that the aging is the key property that decides whether to increase or decrease sensing intervals. Second, inspired by our analytical work, we develop a near-optimal Wi-Fi sensing algorithm, WiSAG, and show that WiSAG outperforms other algorithms through the extensive trace-driven simulations.

The study on Wi-Fi sensing algorithms includes the ones that use surrounding information [13]–[16]. In some cases, such algorithms may outperform WiSAG, which does not use the extra information. However, due to the additional overheads for using them, our focus is first to study the sensing patterns without surrounding information by figuring out which factor is the key to the optimal blind sensing. We believe that WiSAG is widely beneficial in current smartphones, most of which also use a blind sensing policy [13]. It is left as a future work to extend our framework in WiSAG to account for the advantage of the surrounding information.

Appendix

A. Proof of Theorem 1

To simplify the exposition, we first denote the reciprocal of $I(t)$ by: $\lambda(t) \triangleq 1/I(t)$.

(i) Necessity. Let $F(\lambda(t))$ be the functional in (xOPT), i.e.,

$$F(\lambda(t)) = \int_0^\infty \left\{ c_{\mathrm{s}} \lambda(t) \overline{F}_X(t) + \gamma r_w l\left(\frac{1}{2\lambda(t)}\right) f_X(t) \right\} \mathrm{d}t.$$

From the functional derivative techniques in [30] and [34], by differentiating the functional F w.r.t. $\lambda(t)$ and setting it to zero, we obtain

$$\begin{aligned} \frac{\partial F}{\partial \lambda(t)} &= \frac{\partial}{\partial \lambda} \left\{ c_{\mathrm{s}} \lambda(t) \overline{F}_X(t) + \gamma r_w l\left(\frac{1}{2\lambda(t)}\right) f_X(t) \right\} \\ &= c_{\mathrm{s}} \overline{F}_X(t) - \gamma r_w \frac{f_X(t)}{2\lambda(t)^2} l'\left(\frac{1}{2\lambda(t)}\right) = 0. \end{aligned} \tag{22}$$

By noting that $r_X(t) = f_X(t)/\overline{F}_X(t)$, $l'(x) = \overline{F}_Y(t)$ from (7), and $\lambda(t) = 1/I(t)$, (11) follows from (22).

(ii) Sufficiency. The necessary condition in (11) is also sufficient if the functional F is convex [35], i.e.,

$$\alpha F(\lambda(t)) + (1-\alpha)F(\theta(t)) \geq F(\alpha\lambda(t) + (1-\alpha)\theta(t))$$

for any two functions $\lambda(t), \theta(t)$ and $\alpha \in (0,1)$. This is equivalent to

$$\int_0^\infty \left\{\alpha l\left(\frac{1}{2\lambda(t)}\right) + (1-\alpha) l\left(\frac{1}{2\theta(t)}\right)\right\} f_X(t)\mathrm{d}t \geq \int_0^\infty \left\{l\left(\frac{1}{2(\alpha\lambda(t)+(1-\alpha)\theta(t)}\right)\right\} f_X(t)\mathrm{d}t \quad (23)$$

which holds if and only if $h(x) := l(1/2x)$ is convex in $x > 0$. Now, the condition $h''(x) > 0$ reads as

$$\frac{\mathrm{d}^2}{\mathrm{d}x^2}h(x) = \frac{1}{x^3}\left[\overline{F}_Y\left(\frac{1}{2x}\right) - \frac{1}{4x} f_Y\left(\frac{1}{2x}\right)\right] > 0.$$

By replacing x with $\lambda(t)$ and setting $1/\lambda(t) = I(t)$, we get (12). This completes the proof.

B. Proof of Theorem 2

For the sake of notational brevity, we first denote the reciprocal of $I(t)$ by: $\lambda(t) \triangleq 1/I(t)$, and $\widetilde{C}_2$ by the approximated form of the objective in (16). For ease of development, put the approximated form of the objective $\widetilde{C}_2$ as $\frac{K(\lambda(t))}{L(\lambda(t))}$, where $K(\lambda(t))$ and $L(\lambda(t))$ are denoted as follows:

$$K(\lambda(t)) \triangleq \int_0^\infty c_\mathrm{s}\lambda(t)\bar{F}_X(t)\mathrm{d}t \quad (24)$$

$$L(\lambda(t)) \triangleq \int_0^\infty r_w g\left(\frac{1}{2\lambda(t)}\right) f_X(t)\mathrm{d}t. \quad (25)$$

By the definition of functional derivative [30], we compute a functional derivative of nonlocal functional $\widetilde{C}_2$ as follows:

$$\begin{aligned}\frac{\delta\widetilde{C}_2(\lambda(t))}{\delta\lambda(y)} &= \lim_{\epsilon\to 0}\frac{\widetilde{C}_2(\lambda(t)+\epsilon\delta(t-y)) - \widetilde{C}_2(\lambda(t))}{\epsilon}\\ &= \lim_{\epsilon\to 0}\frac{1}{\epsilon}\left\{\frac{K(\lambda(t)+\epsilon\delta(t-y))}{L(\lambda(t)+\epsilon\delta(t-y))} - \frac{K(\lambda(t))}{L(\lambda(t))}\right\}\\ &= \lim_{\epsilon\to 0}\frac{1}{L(\lambda(t)+\epsilon\delta(t-y))L(\lambda(t))}\\ &\quad\times\left\{L(\lambda(t))\frac{K(\lambda(t)+\epsilon\delta(t-y)) - K(\lambda(t))}{\epsilon}\right.\\ &\quad\left. - K(\lambda(t))\frac{L(\lambda(t)+\epsilon\delta(t-y)) - L(\lambda(t))}{\epsilon}\right\}\\ &= \frac{1}{L(\lambda)^2}\left\{\frac{\delta K(\lambda)}{\delta\lambda(y)}L(\lambda) - \frac{\delta L(\lambda)}{\delta\lambda(y)}K(\lambda)\right\}. \quad (26)\end{aligned}$$

Then, we compute $\frac{\delta}{\delta\lambda}K(\lambda)$ and $\frac{\delta}{\delta\lambda}L(\lambda)$

$$\frac{\delta}{\delta\lambda}K(\lambda) = \frac{\partial}{\partial\lambda}c_\mathrm{s}\lambda\overline{F}_X(t) = c_\mathrm{s}\overline{F}_X(t) \quad (27)$$

$$\frac{\delta}{\delta\lambda}L(\lambda) = \frac{\partial}{\partial\lambda}r_w g(\frac{1}{2\lambda})f_X(t) = \frac{r_w\overline{F}_Y\left(\frac{1}{2\lambda}\right)f_X(t)}{2\lambda^2}. \quad (28)$$

Equations (26)–(28) lead to the following equation:

$$\frac{\delta\widetilde{C}_2}{\delta\lambda} = \frac{L(\lambda)c_\mathrm{s}\overline{F}_X(t) - K(\lambda)\frac{r_w\overline{F}_Y(\frac{1}{2\lambda})f_X(t)}{2\lambda^2}}{(L(\lambda))^2}. \quad (29)$$

Then, putting the right-hand side of (29) zero

$$\frac{\overline{F}_Y(\frac{1}{2\lambda(t)})}{\lambda(t)^2} = \frac{2c_\mathrm{s}\overline{F}_X(t)}{r_w f_X(t)}\frac{L(\lambda)}{K(\lambda)} = \frac{2}{r_X(t)}B \quad (30)$$

where $r(t)$ is a failure rate [20] of distribution F_X and $B = \frac{\int_0^\infty g(1/2\lambda(t))f_X(t)\mathrm{d}t}{\int_0^\infty \lambda(t)\bar{F}_X(t)\mathrm{d}t}$. Note that the unknown coefficient B does not depend on t because both denominator and numerator of B are functionals that have scalar values. Then, replacing $\lambda(t)$ to $I(t)$, we arrive at the (17)

REFERENCES

[1] Cisco, "Cisco Visual Networking Index: Global mobile data traffic forecast update," Feb. 2011.

[2] K. Lee, I. Rhee, J. Lee, S. Chong, and Y. Yi, "Mobile data offloading: How much can WiFi deliver?," in *Proc. ACM CoNEXT*, 2010, Art. no. 26.

[3] A. Balasubramanian, R. Mahajan, and A. Venkataramani, "Augmenting mobile 3G using WiFi," in *Proc. ACM MobiSys*, 2010, pp. 209–222.

[4] M.-R. Ra *et al.*, "Energy-delay tradeoffs in smartphone applications," in *Proc. ACM MobiSys*, 2010, pp. 255–270.

[5] Apple, "iCloud," 2011 [Online]. Available: http://www.apple.com/icloud/

[6] Microsoft, "Microsoft Pocket Outlook," [Online]. Available: http://www.microsoft.com/windowsmobile/en-us/downloads/microsoft/office-outlook-mobile.mspx

[7] USC/ENL, "Vcaps: Urban tomography project," 2015 [Online]. Available: http://nsl.cs.usc.edu/Projects/UrbanTomography

[8] F. Baccelli and J. Bolot, "Modeling the economic value of the location data of mobile users," in *Proc. IEEE INFOCOM*, Apr. 2011, pp. 1467–1475.

[9] Devicespace, "Research on usage and trends," Wi-Fi Report, Jun. 2011.

[10] R. Friedman, A. Kogan, and Y. Krivolapov, "On power and throughput tradeoffs of WiFi and Bluetooth in smartphones," in *Proc. IEEE INFOCOM*, 2011, pp. 900–908.

[11] A. Rahmati and L. Zhong, "Context-for-wireless: context-sensitive energy-efficient wireless data transfer," in *Proc. ACM MobiSys*, 2007, pp. 165–178.

[12] N. Balasubramanian, A. Balasubramanian, and A. Venkataramani, "Energy consumption in mobile phones: A measurement study and implications for network applications," in *Proc. ACM IMC*, 2009, pp. 280–293.

[13] K. Kim, A. Min, D. Gupta, P. Mohapatra, and J. Singh, "Improving energy efficiency of Wi-Fi sensing on smartphones," in *Proc. IEEE INFOCOM*, Apr. 2011, pp. 2930–2938.

[14] H. Wu, K. Tan, and J. Liu, "Footprint: Cellular assisted Wi-Fi AP discovery on mobile phones for energy saving," in *Proc. ACM WINTECH*, 2009, pp. 67–76.

[15] R. Zhou, Y. Xiong, G. Xing, L. Sun, and J. Ma, "ZiFi: Wireless LAN discovery via ZigBee interference signatures," in *Proc. ACM MobiCom*, 2010, pp. 49–60.

[16] G. Ananthanarayanan and I. Stoica, "Blue-Fi: Enhancing Wi-Fi performance using Bluetooth signals," in *Proc. ACM MobiSys*, 2009, pp. 249–262.

[17] C. Research, "iPhone 4 owners tell us what they really think about their smart phones," ChangeWave Research Report, Aug. 2010.

[18] W. Wang, M. Motani, and V. Srinivasan, "Opportunistic energy-efficient contact probing in delay-tolerant applications," *IEEE/ACM Trans. Netw.*, vol. 17, no. 5, pp. 1592–1605, Oct. 2009.

[19] R. T. Marler and J. S. Arora, "Survey of multi-objective optimization methods for engineering," *Struct. Multidiscipl. Optimiz.*, vol. 26, no. 6, pp. 369–395, 2004.

[20] C.-D. Lai and M. Xie, *Stochastic Ageing and Dependence for Reliability*. New York, NY, USA: Springer, 2006.

[21] M. Kim and D. Kotz, "Periodic properties of user mobility and access-point popularity," *Journal of Personal and Ubiquitous Comput.*, vol. 11, no. 6, pp. 465–479, Aug. 2007.

[22] W. Hsu, T. Spyropoulos, K. Psounis, and A. Helmy, "Modeling time-variant user mobility in wireless mobile networks," in *Proc. IEEE INFOCOM*, 2007, pp. 758–766.

[23] R. L. Keeney and H. Raiffa, *Decisions With Multiple Objectives: Preferences and Value Trade-Offs*. Cambridge, U.K.: Cambridge Univ. Press, 1993.
[24] C. Joe-Wong, S. Sen, and S. Ha, "Offering supplementary wireless technologies: Adoption behavior and offloading benefits," in *Proc. IEEE INFOCOM*, 2013, pp. 1061–1069.
[25] H. Cai and D. Y. Eun, "Aging rules: What does the past tell about the future in mobile ad-hoc networks?," in *Proc. ACM MobiHoc*, 2009, pp. 115–124.
[26] N. Kaio and S. Osaki, "Comparison of inspection policies," *J. Oper. Res. Soc.*, vol. 40, pp. 499–503, 1989.
[27] R. E. Barlow, L. C. Hunter, and F. Proschan, "Optimum checking procedures," *J. SIAM*, vol. 11, pp. 1078–1095, 1963.
[28] S. Kim and H. David, "On the dependence structure of order statistics and concomitants of order statistics," *J. Statist. Planning Inference*, vol. 24, pp. 363–368, 1990.
[29] J.-Y. Le Boudec, *Performance Evaluation of Computer and Communication Systems*. Lasuanne, Switzerland: EPFL Press, 2010.
[30] I. Gelfand and S. Fomin, *Calculus of Variations*. Upper Saddle River, NJ, USA: Prentice-Hall, 1963.
[31] V. Conan, J. Leguay, and T. Friedman, "Characterizing pairwise inter-contact patterns in delay tolerant networks," in *Proc. 1st Int. Conf. Auton. Comput. Commun. Syst.*, 2007, Art. no. 19.
[32] W. T. Eadie, M. Roos, and F. James, *Statistical Methods in Experimental Physics*. Amsterdam, The Netherlands: Elsevier, 1971.
[33] H. Falaki and S. Keshav, "Trace-based analysis of Wi-Fi scanning strategies," in *Proc. ACM MobiCom*, 2008, pp. 73–76, Poster.
[34] J. B. Keller, "Optimum checking schedulers for systems subject to random failure," *Manage. Sci.*, vol. 21, pp. 256–260, 1974.
[35] D. G. Luenberger, *Optimization by Vector Space Methods*. New York, NY, USA: Wiley, 1969.

Jaeseong Jeong received the B.S., M.S., and Ph.D. degrees in electrical engineering from Korea Advanced Institute of Science and Technology (KAIST), Daejeon, Korea, in 2008, 2010, and 2014, respectively.

He is currently a Postdoctoral Researcher with the Automatic Control Department, KTH, Stockholm, Sweden. His research interests include human mobility/behavior analysis and prediction, protocol design, and implementation for mobile networks and vehicular sensor networks.

Yung Yi received the B.S. and M.S. degrees in computer science and engineering from Seoul National University, Seoul, Korea, in 1997 and 1999, respectively, and the Ph.D. degree in electrical and computer engineering from the University of Texas at Austin, Austin, TX, USA, in 2006.

From 2006 to 2008, he was a Post-Doctoral Research Associate with the Department of Electrical Engineering, Princeton University, Princeton, NJ, USA. Now, he is an Associate Professor with the Department of Electrical Engineering, Korea Advanced Institute of Science and Technology (KAIST), Daejeon, Korea. His current research interests include the design and analysis of computer networking and wireless communication systems, especially congestion control, scheduling, and interference management, with applications in wireless ad hoc networks, broadband access networks, economic aspects of communication networks (a.k.a. network economics), and green networking systems.

Dr. Yi is now an Associate Editor of the IEEE/ACM TRANSACTIONS ON NETWORKING, *Journal of Communication Networks*, and *Computer Communications*. He was the recipient of two Best Paper awards at IEEE SECON 2013 and ACM MobiHoc 2013.

Jeong-Woo Cho received the B.S., M.S., and Ph.D. degrees in electrical engineering and computer science from Korea Advanced Institute of Science and Technology (KAIST), Daejeon, Korea, in 2000, 2002, and 2005, respectively.

From 2005 to 2007, he was with the Telecommunication R&D Center, Samsung Electronics, Suwon, Korea, as a Senior Engineer. From 2007 to 2010, he held postdoctoral positions with the School of Computer and Communication Sciences, École Polytechnique Fédérale de Lausanne (EPFL), Lausanne, Switzerland, and the Centre for Quantifiable Quality of Service in Communication Systems, Norwegian University of Science and Technology (NTNU), Trondheim, Norway. He is now an Assistant Professor with the School of Information and Communication Technology, KTH Royal Institute of Technology, Stockholm, Sweden. His current research interests include performance evaluation in various networks such as wireless local area network, delay-tolerant network, and peer-to-peer network.

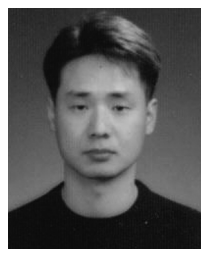

Do Young Eun (M'03–SM'15) received the B.S. and M.S. degrees in electrical engineering from Korea Advanced Institute of Science and Technology (KAIST), Daejeon, Korea, in 1995 and 1997, respectively, and the Ph.D. degree in electrical and computer engineering from Purdue University, West Lafayette, IN, USA, in 2003.

Since 2003, he has been with the Department of Electrical and Computer Engineering, North Carolina State University, Raleigh, NC, USA, where he is currently an Associate Professor. His research interests include network modeling and performance analysis, mobile ad hoc/sensor networks, mobility modeling, social networks, and graph sampling.

Dr. Eun has been a member of the Technical Program Committee of various conferences including IEEE INFOCOM, ICC, GLOBECOM, ACM MobiHoc, and ACM SIGMETRICS. He is currently on the Editorial Board of the IEEE/ACM TRANSACTIONS ON NETWORKING and *Computer Communications*, and was TPC Co-Chair of WASA 2011. He received the Best Paper awards in the IEEE ICCCN 2005 and IEEE IPCCC 2006, and the National Science Foundation CAREER Award 2006. He supervised and coauthored a paper that received the Best Student Paper Award in ACM MobiCom 2007.

Song Chong (S'93–M'95) received the B.S. and M.S. degrees from Seoul National University, Seoul, Korea, in 1988 and 1990, and the Ph.D. degree from the University of Texas at Austin, Austin, TX, USA, in 1995, all in electrical engineering.

He is a Professor with the Department of Electrical Engineering, Korea Advanced Institute of Science and Technology (KAIST), Daejeon, Korea, and was the Head of Communication and Computing Division of the department in 2009 to 2010. He is the Founding Director of KAIST-LGE 5G Mobile Communications and Networking Research Center funded by LG Electronics. Prior to joining KAIST in 2000, he was with the Performance Analysis Department, AT&T Bell Laboratories, Holmdel, NJ, USA, as a Member of Technical Staff. His current research interests include wireless networks, mobile networks and systems, network data analytics, distributed algorithms, and cross-layer control and optimization.

Prof. Chong is currently an Editor of the IEEE/ACM TRANSACTIONS ON NETWORKING, IEEE TRANSACTIONS ON MOBILE COMPUTING, and IEEE TRANSACTIONS ON WIRELESS COMMUNICATIONS. He served as the Technical Program Committee Co-Chair of IEEE SECON 2015 and has served on the Technical Program Committee of a number of leading international conferences including IEEE INFOCOM, ACM MobiCom, ACM CoNEXT, ACM MobiHoc, and IEEE ICNP. He serves on the Steering Committee of WiOpt and was the General Chair of WiOpt 2009. He received the IEEE William R. Bennett Prize in 2013, and the IEEE SECON Best Paper Award in 2013.